Pentaquarks from hidden-strange to hidden-bottom systems

Hongxia Huang (黄虹霞)
Nanjing Normal University

6th workshop on the XYZ particles
Fudan University，2020.1.11-2020.1.13

Outline

I. Introduction

II. Quark model and calculation methods

III. Hidden-charm pentaquarks

IV. Hidden-bottom pentaquarks

V. Hidden-strange pentaquarks

VI. Summary

I. Introduction

➢ Experimental results

- **2015** LHCb Collaboration, Phys. Rev. Lett. 115, 072001

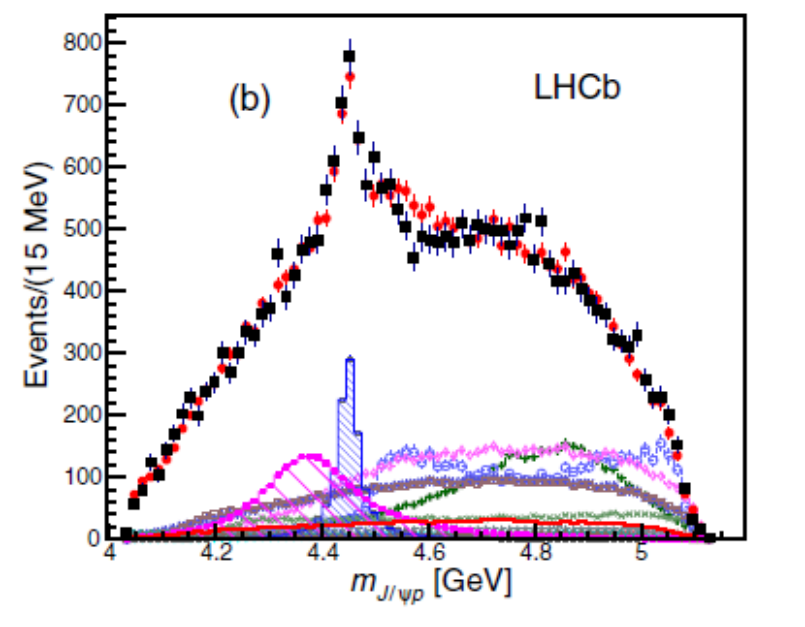

- The two P_c^+ states are found to have **masses and widths** of
  $M_{P_c\,(4380)} = 4380 \pm 8 \pm 29$ MeV
  $\Gamma_{P_c\,(4380)} = 205 \pm 18 \pm 86$MeV
  $M_{P_c\,(4450)} = 4449.8 \pm 1.7 \pm 2.5$ MeV
  $\Gamma_{P_c\,(4450)} = 39 \pm 5 \pm 19$ MeV

- The preferred **spin-parity J^P** are of opposite values, with one state having spin 3/2 and the other 5/2.

- **2019** LHCb Collaboration, Phys. Rev. Lett. 122 222001

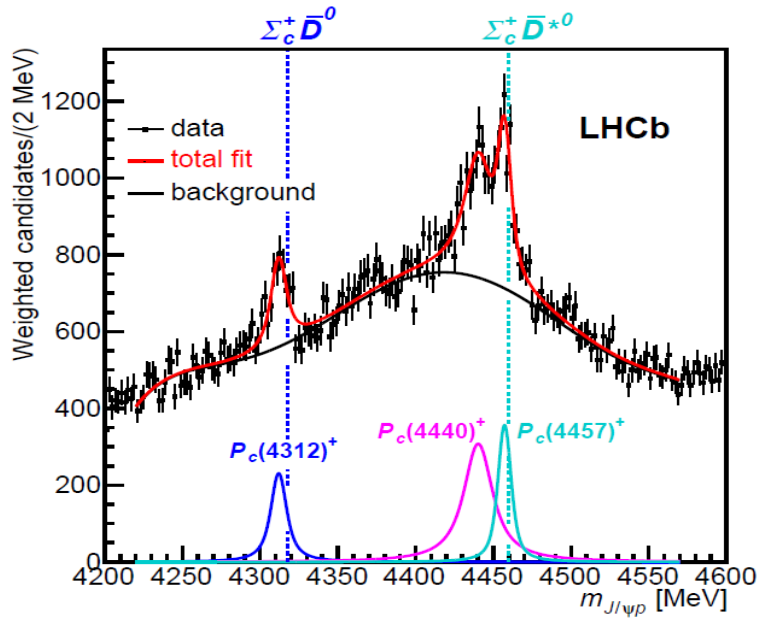

Figure 6: Fit to the $\cos\theta_{P_c}$-weighted $m_{J/\psi p}$ distribution with three BW amplitudes and a sixth-order polynomial background. This fit is used to determine the central values of the masses and widths of the P_c^+ states. The mass thresholds for the $\Sigma_c^+\bar{D}^0$ and $\Sigma_c^+\bar{D}^{*0}$ final states are superimposed.

- The *Pc*(4312) was discovered with 7.3σ significance by analyzing the *J/ψp* invariant mass spectrum.
- The previously reported *Pc*(4450) structure was resolved at 5.4σ significance into two narrow states: the *Pc*(4440) and *Pc*(4457).

Table 1: Summary of P_c^+ properties. The central values are based on the fit displayed in Fig. 6.

State	M [MeV]	Γ [MeV]	(95% CL)	$\mathcal{R}$ [%]
$P_c(4312)^+$	$4311.9 \pm 0.7^{+6.8}_{-0.6}$	$9.8 \pm 2.7^{+3.7}_{-4.5}$	(< 27)	$0.30 \pm 0.07^{+0.34}_{-0.09}$
$P_c(4440)^+$	$4440.3 \pm 1.3^{+4.1}_{-4.7}$	$20.6 \pm 4.9^{+8.7}_{-10.1}$	(< 49)	$1.11 \pm 0.33^{+0.22}_{-0.10}$
$P_c(4457)^+$	$4457.3 \pm 0.6^{+4.1}_{-1.7}$	$6.4 \pm 2.0^{+5.7}_{-1.9}$	(< 20)	$0.53 \pm 0.16^{+0.15}_{-0.13}$

➢ Theoretical studies

- After LHCb's Pc results (2015)

1) Loosely bound molecular baryon-meson pentaquark states:

M. Karliner and J. L. Rosner, Phys. Rev. Lett. 115, 122001 (2015).

R. Chen, X. Liu, X.-Q. Li, S.-L. Zhu, Phys.Rev.Lett. 115, no.13, 132002 (2015).

H. X. Chen, W. Chen, X. Liu, T.G. Steele and S. L. Zhu, Phys.Rev.Lett. 115, no.17, 172001 (2015) .

L. Roca, J. Nieves and E. Oset, Phys. Rev. D 92, 094003 (2015).

J. He, Phys.Lett. B753, 547-551 (2016) .

H. X. Huang, C. R. Deng, J. L. Ping, and F. Wang, Eur. Phys. J. C 76, 624 (2016).

H. X. Huang and J. L. Ping, Phys. Rev. D 99, 014010 (2019).

G. Yang and J. L. Ping, Phys. Rev. D 95, 010014 (2017).

A. Feijoo, V. K. Magas, A. Ramos and E. Oset, Phys. Rev. D 95, no.3, 039905 (2017).

and others.

2) Tightly bound pentaquark states

L. Maiani, A.D. Polosa, and V. Riquer, Phys.Lett. B 749, 289-291 (2015).

R. F. Lebed, Phys.Lett. B 749, 454-457 (2015).

G.-N. Li, X.-G. He, M. He, JHEP 1512, 128 (2015).

Z.-G. Wang, Eur. Phys. J. C 76, no.2, 70 (2016).

R. Zhu and C. F. Qiao, Phys.Lett. B 756, 259 (2016).
V. V. Anisovich et al., arXiv:1507.07652.
R. Ghosh, A. Bhattacharya, and B. Chakrabarti, Phys. Part. Nucl. Lett. 14, 550 (2017).

and others.

3) Peaks due to triangle-diagram processes

F.-K. Guo, U.-G. Meißner, W. Wang, and Z. Yang, Phys. Rev. D 92, 071502(R) (2015).
U.-G. Meißner and J. A. Oller, Phys. Lett. B 751, 59 (2015).
X.-H. Liu, Q. Wang, and Q. Zhao, Phys. Lett. B 757, 231 (2016).
Q. Wang, X.-H. Liu, and Q. Zhao, Phys.Rev. D92, 034022 (2015).
M. Mikhasenko, arXiv:1507.06552.

and others.

- Immediately after LHCb's Pc results (2019)

R. Chen, X. Liu, Z.-F. Sun, and S.-L. Zhu, arXiv:1903.11013 [hep-ph].

F. K. Guo, H. J. Jing, U.-G. Meissner, and S. Sakai, arXiv:1903.11503 [hep-ph].

J. He, arXiv:1903.11872 [hep-ph].

Hua-Xing Chen , Wei Chen, Shi-Lin Zhu, arXiv: 1903.11001 [hep-ph].

H. X. Huang, J. He, and J. L. Ping, arXiv: 1904.00221 [hep-ph].

C. J. Xiao, Y. Huang, Y. B. Dong, L. S. Geng, and D. Y. Chen, arXiv:1904.00872 [hep-ph].

M. Z. Liu, Y. W. Pan, F. Z. Peng, M. S. Sanchez, L. S. Geng, A. Hosaka, and M. P. Valderrama, , Phys. Rev. Lett. **122**, 242001 (2019)

and others.

- Some early studies

J. J. Wu, R. Molina, E. Oset and B. S. Zou, Phys. Rev. Lett. **105**, 232001 (2010) [arXiv:1007.0573 [nucl-th]].

J. J. Wu, R. Molina, E. Oset and B. S. Zou, Phys. Rev. C **84**, 015202 (2011) [arXiv:1011.2399 [nucl-th]].

J. J. Wu, T.-S. H. Lee and B. S. Zou, Phys. Rev. C **85**, 044002 (2012) [arXiv:1202.1036 [nucl-th]].

Z. C. Yang, Z. F. Sun, J. He, X. Liu and S. L. Zhu, Chin. Phys. C **36**, 6 (2012) [arXiv:1105.2901 [hep-ph]].

and others.

➢ Nϕ

- The Nϕ bound state was first studied by H. Gao .

PRC 63 (2001) 022201(R)

The QCD van der Waals attractive potential is strong enough to bind a ϕ meson onto a nucleon inside a nucleus to form a bound state.

- The feasibility of experimental search for the Nϕ bound state at Jefferson Lab was demonstrated by H. Gao .

PRC 75 (2007) 058201

- Measurement of coherent ϕ-meson photoproduction from the deuteron.

CLAS Collaboration, PRC 76 (2007) 052202(R)
PLB 680 (2009) 417-422, PLB 696 (2011) 338-342

- The Nϕ was a quasi-bound state in the extended chiral SU(3) quark model.

PRC 73 (2006) 025207

➢ Our work

1) Hidden-charm pentaquark

2) Hidden-bottom pentaquark

Eur. Phys. J. C. 76, 624 (2016), arXiv: 1510.04648.

Phys. Rev. D. 99, 014010 (2019) , arXiv: 1811.04260.

3) Hidden-strange pentaquark

Phys. Rev. C. 95, 055202 (2017) , arXiv: 1701.03210.

Phys. Rev. D. 97, 094019 (2018) , arXiv: 1803.05267.

II. Quark model and calculation methods

➢ Quark delocalization color screening model (QDCSM)

- QDCSM was developed by Nanjing-Los Alamos collaboration in1990s aimed to multi-quark study. (PRL 69, 2901, 1992)
- Two new ingredients (based on quark cluster model configuration):

  quark delocalization (orbital excitation)

  color screening (color structure)
- Apply to the study of baryon-baryon interaction and dibaryons

  deuteron, d, NN, NΛ, NΩ, …*
- Apply to the study of baryon-meson interaction and pentaquarks

  NK, Npi, …

$$H=\sum_{i=1}^{5}\left(m_i+\frac{p_i^2}{2m_i}\right)-T_c+\sum_{i<j}[V^G(r_{ij})+V^\chi(r_{ij})+V^C(r_{ij})],$$

$$V^G(r_{ij})=\frac{1}{4}\alpha_s\lambda_i\cdot\lambda_j\left[\frac{1}{r_{ij}}-\frac{\pi}{2}\left(\frac{1}{m_i^2}+\frac{1}{m_j^2}+\frac{4\sigma_i\cdot\sigma_j}{3m_im_j}\right)\delta(r_{ij})-\frac{3}{4m_im_jr_{ij}^3}S_{ij}\right],$$

$$V^\chi(r_{ij})=\frac{1}{3}\alpha_{ch}\frac{\Lambda^2}{\Lambda^2-m_\chi^2}m_\chi\left\{\left[Y(m_\chi r_{ij})-\frac{\Lambda^3}{m_\chi^3}Y(\Lambda r_{ij})\right]\sigma_i\cdot\sigma_j+\left[H(m_\chi r_{ij})-\frac{\Lambda^3}{m_\chi^3}H(\Lambda r_{ij})\right]S_{ij}\right\}\mathbf{F}_i\cdot\mathbf{F}_j,\qquad \chi=\pi,K,\eta,$$

$$V^C(r_{ij})=-a_c\lambda_i\cdot\lambda_j[f(r_{ij})+V_0],$$

$$f(r_{ij})=\begin{cases} r_{ij}^2 & \text{if } i,j \text{ occur in the same baryon orbit,}\\ \frac{1-e^{-\mu_{ij}r_{ij}^2}}{\mu_{ij}} & \text{if } i,j \text{ occur in different baryon orbits,}\end{cases}$$

$$S_{ij}=\frac{(\sigma_i\cdot\mathbf{r}_{ij})(\sigma_j\cdot\mathbf{r}_{ij})}{r_{ij}^2}-\frac{1}{3}\sigma_i\cdot\sigma_j, \tag{1}$$

$$\psi_\alpha(\boldsymbol{s}_i,\epsilon)=(\phi_\alpha(\boldsymbol{s}_i)+\epsilon\phi_\alpha(-\boldsymbol{s}_i))/N(\epsilon),$$
$$\psi_\beta(-\boldsymbol{s}_i,\epsilon)=(\phi_\beta(-\boldsymbol{s}_i)+\epsilon\phi_\beta(\boldsymbol{s}_i))/N(\epsilon),$$

$$N(\epsilon)=\sqrt{1+\epsilon^2+2\epsilon e^{-s_i^2/4b^2}},$$

$$\phi_\alpha(\boldsymbol{s}_i)=\left(\frac{1}{\pi b^2}\right)^{3/4}e^{-\frac{1}{2b^2}(\boldsymbol{r}_\alpha-\frac{2}{5}\boldsymbol{s}_i/2)^2},$$

$$\phi_\beta(-\boldsymbol{s}_i)=\left(\frac{1}{\pi b^2}\right)^{3/4}e^{-\frac{1}{2b^2}(\boldsymbol{r}_\beta+\frac{3}{5}\boldsymbol{s}_i/2)^2}.$$

➢ Calculation methods

(1) Resonating group method (RGM)

In RGM, the multi-quark wave function is approximated by the cluster wave function,

$$\psi(\xi_1, \xi_2, R) = \mathcal{A}[\phi(\xi_1)\phi(\xi_2)\chi(R)]$$

The internal motions of clusters are frozen and the relative motion wave function satisfies the following RGM equation

$$\int H(R'', R')\chi(R')dR' = E\int N(R'', R')\chi(R')dR'$$

$$\left\{ \begin{array}{c} H(R'', R') \\ N(R'', R') \end{array} \right\} = \left\langle A[\phi_1\phi_2\delta(R - R'')] \left| \left\{ \begin{array}{c} H \\ 1 \end{array} \right\} \right| A[\phi_1\phi_2\delta(R - R')] \right\rangle$$

RGM equation

$$\int L(R'', R')\chi(R')dR' = 0$$

where

$$L(R'', R') = H(R'', R') - EN(R'', R')$$

$$= [-\frac{\nabla^2_{R'}}{2\mu} + V^D_{rel}(R') - E_{rel}]\delta(R'' - R') + H^{EX}(R'', R') - EN^{EX}(R'', R')$$

(2) Generating coordinates method (GCM)

Extending the relative motion wave function to the Gaussian function:

$$\chi(\vec{R}) = \sum_i C_i \chi_i(\vec{R}) = (\frac{3}{2\pi b^2})^{3/4} \sum_i C_i e^{-\frac{3}{4}(\vec{R}-\vec{S}_i)^2/b^2}$$

$$\phi_C(\vec{R_C}) = (\frac{6}{\pi b^2})^{\frac{3}{4}} e^{-\frac{3}{b^2}(\vec{R_c})^2}$$

$$\Psi_{6q} = A \sum_i C_i \prod_{\alpha=1}^{3} \phi_\alpha(\vec{S}_i) \prod_{\beta=4}^{6} \phi_\beta(-\vec{S}_i)$$
$$[\eta_{I_1 s_1}(B_1)\eta_{I_2 s_2}(B_2)]^{IS}[\chi_c(B_1)\chi_c(B_2)]^{[\sigma]}$$

$$\Psi_{6q} = A\sum_{k}\sum_{i,L_k} C_{k,i,L_k}\int \frac{d\Omega_{S_i}}{\sqrt{4\pi}} \prod_{\alpha=1}^{3}\psi_\alpha(\vec{S}_i,\epsilon)\prod_{\beta=4}^{6}\psi_\beta(-\vec{S}_i,\epsilon)$$
$$[[\eta_{I_{1k}S_{1k}}(B_{1k})\eta_{I_{2k}S_{2k}}(B_{2k})]^{IS_k}Y^{L_k}(\hat{\vec{S}}_i)]^J[\chi_C(B_1)\chi_c(B_2)]^{[\sigma]}$$

$$\int H(\vec{R},\vec{R}')\chi(\vec{R}')d\vec{R}' = E\int N(\vec{R},\vec{R}')\chi(\vec{R}')d\vec{R}'$$

$$\Downarrow$$

$$\sum_{j,k,L_k} C_{j,k,L_k} H_{i,j}^{k',L'_k,k,L_k} = E\sum_{j,k,L_k} C_{j,k,L_k} N_{i,j}^{k',L'_k,k,L_k}\delta_{L'_k,L_k}$$

(2) Kohn-Hulthen-Kato(KHK) variational method

$$u_t(R) = \sum_{i=0}^{n} c_i u_i(R)$$

$$u_i(R) = \begin{cases} \alpha_i u_i^{(in)}(R), & R < R_c, \\ (h_L^{(-)}(k,R) + s_i h_L^{(+)}(k,R))R, & R > R_c \end{cases}$$

$$\frac{u_i^{(in)}(R)}{R} = \sqrt{4\pi}\left(\frac{3}{2\pi b^2}\right)^{\frac{3}{4}} e^{-\frac{3}{4b^2}(R^2+r_i^2)} i^L j_L\left(-i\frac{3}{2b^2}Rr_i\right)$$

$$\sum_{i=0}^{n} c_i = 1, \qquad \sum_{i=0}^{n} c_i s_i = S_t.$$

$$c_0 = 1 - \sum_{i=1}^{n} c_i \quad \Rightarrow \quad u_t(R) = u_0(R) + \sum_{i=1}^{n} c_i(u_i(R) - u_0(R))$$

$$\langle \delta\Psi' | H - E | \Psi \rangle = 0$$

$$\sum_{j=1}^{n} \mathcal{L}_{ij} c_j = \mathcal{M}_i, (i = 1 \sim n)$$

$$\mathcal{L}_{ij} = \mathcal{K}_{ij} - \mathcal{K}_{i0} - \mathcal{K}_{0j} + \mathcal{K}_{00},$$

$$\mathcal{M}_i = \mathcal{K}_{00} - \mathcal{K}_{i0}$$

$$\mathcal{K}_{ij} = \langle \phi_A(\xi_A)\phi_B(\xi_B)u_i(R)/R \cdot Y_{LM}(\hat{R}) | H - E | \mathcal{A}[\phi_A(\xi_A)\phi_B(\xi_B)u_j(R)/R \cdot Y_{LM}(\hat{R})] \rangle$$

$$c_i \xrightarrow{\sum_{i=0}^{n} c_i s_i = S_t} S_t \longrightarrow S_L \xrightarrow{S_L = |S_L| e^{2i\delta_L}} \delta_L$$

➢ Some examples

1). d* mass and width in NN scattering

PRC 79 (2009) 024001

N_{ch}	ChQM2		ChQM2a		QDCSM0		QDCSM1		QDCSM3	
	M	Γ	M	Γ	M	Γ	M	Γ	M	Γ
1c	2425	–	2430	–	2413	–	2365	–	2276	–
2cc	2428	17	2433	10	2416	20	2368	20	2278	19
4cc	2413	14	2424	9	2400	14	2357	14	2273	17
10cc	2393	14			–	–	–	–	–	–
10cc′	2353	17			–	–	–	–	–	–
10cc″	2351	21			–	–	–	–	–	–

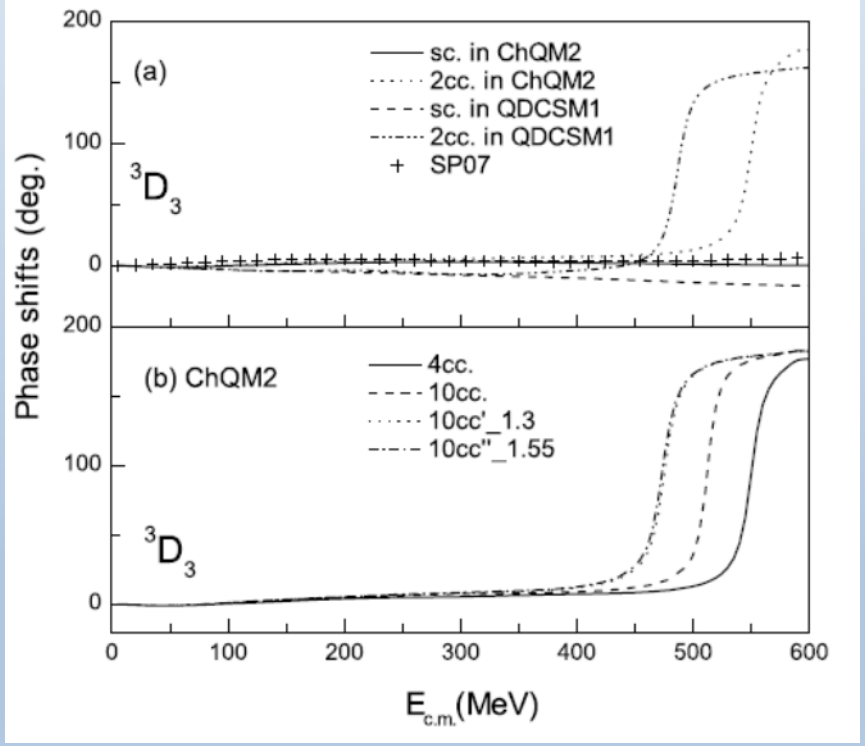

$m = 2.37$ GeV, $\Gamma \approx 70$ MeV and $I(J^P) = 0(3^+)$

2). Δ mass and width in Npi scattering

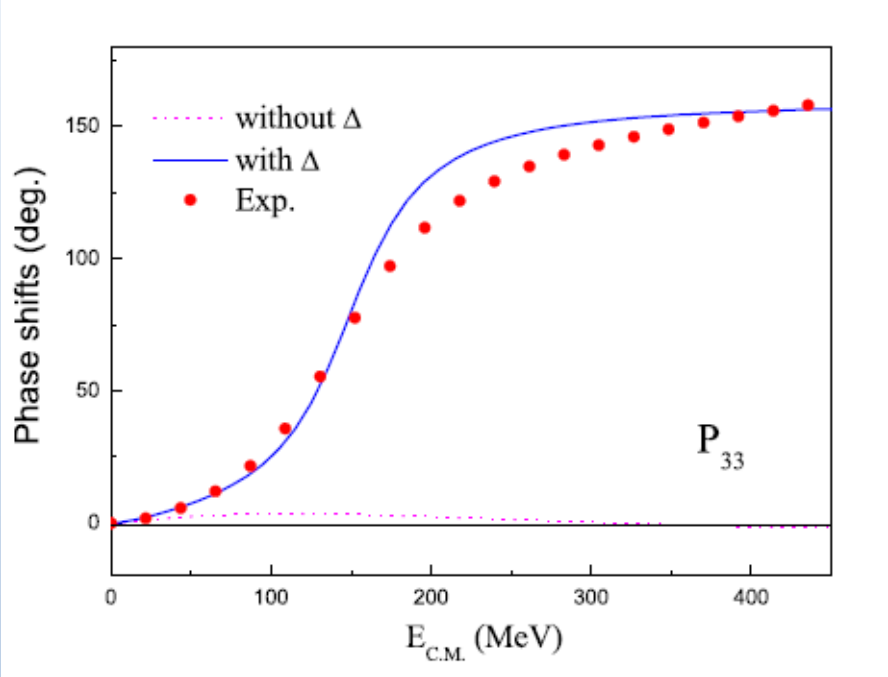

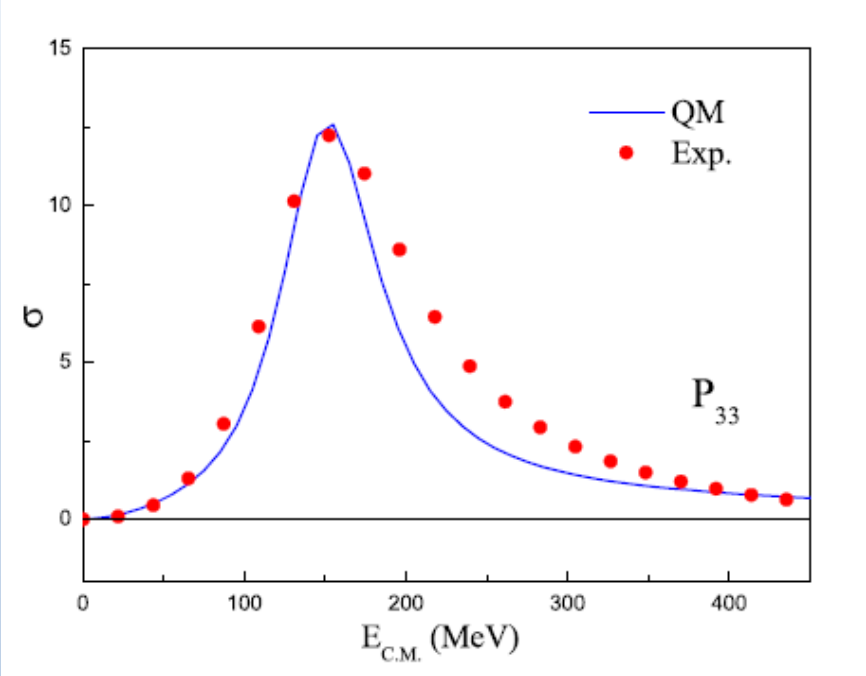

M0=1525 MeV → $M = 1232$ MeV, $\Gamma \sim 90$ MeV

- ✓ The mass of the resonance state will shift by coupling to the open channel. It is better to study the resonances in the scattering process rather than in the limited space.
- ✓ Extending the work to the other pentaquark systems is feasible.

III. Hidden-charm pentaquarks

- The hidden charm pentaquark channels with I=1/2

Table 3 The channels involved in the calculation

$S=\frac{1}{2}$	$N\eta_c$	NJ/ψ	$\Lambda_c D$	$\Lambda_c D^*$	$\Sigma_c D$
	$\Sigma_c D^*$	$\Sigma_c^* D^*$			
$S=\frac{3}{2}$	NJ/ψ	$\Lambda_c D^*$	$\Sigma_c D^*$	$\Sigma_c^* D$	$\Sigma_c^* D^*$
$S=\frac{5}{2}$	$\Sigma_c^* D^*$				

✓ The state with the positive parity is unbound in present calculations.

- The effective potentials

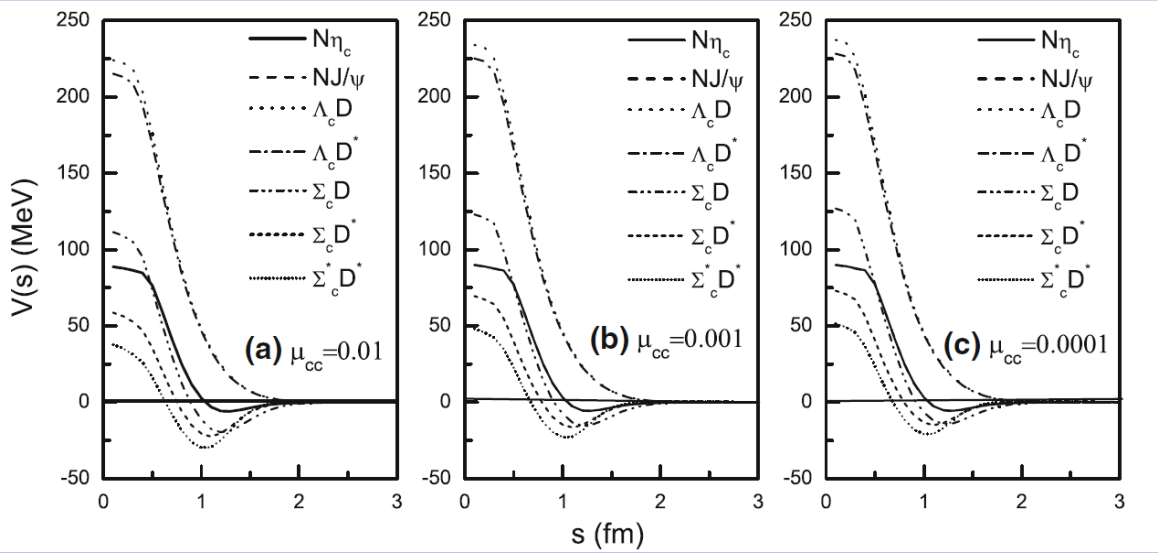

Fig. 1 The potentials of different channels for the $IJ^P = \frac{1}{2}\frac{1}{2}^-$ system

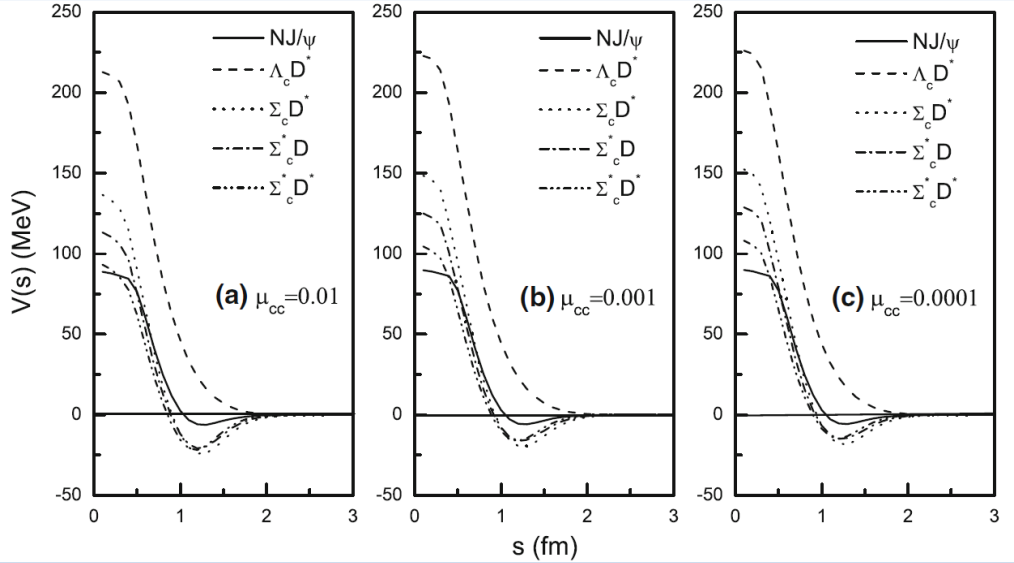

Fig. 2 The potentials of different channels for the $IJ^P = \frac{1}{2}\frac{3}{2}^-$ system

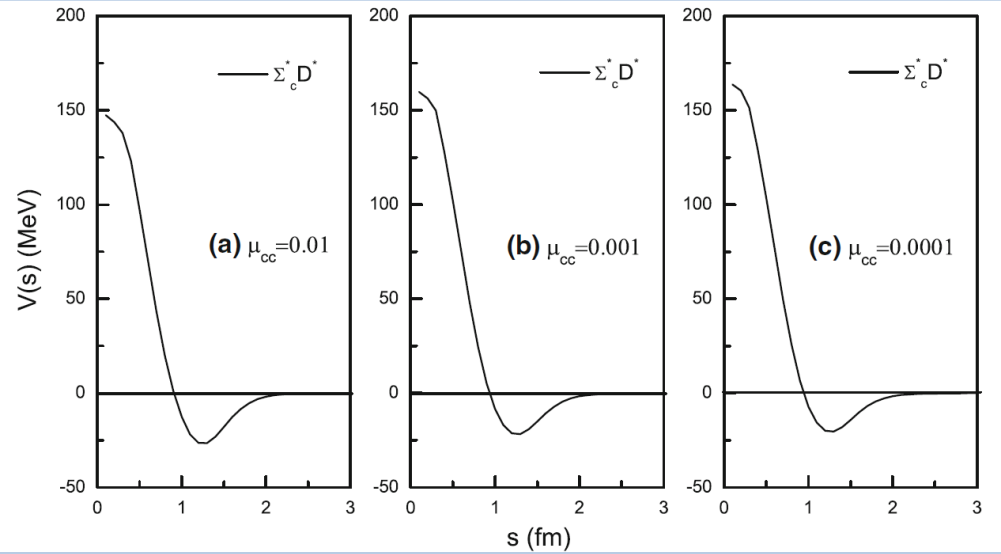

Fig. 3 The potential of a single channel for the $IJ^P = \frac{1}{2}\frac{5}{2}^-$ system

- ✓ The potentials are repulsive between Λc and D/D*. So no bound states or resonances can be formed in these two channels *ΛcD and ΛcD*.*
- ✓ Strong attractions between Σc/Σc* and D/D*.
- ✓ It is possible for Σc/Σc* and D/ D* to form bound states or resonance states.

- The single channel calculation

$J^P = \frac{1}{2}^-$				$J^P = \frac{3}{2}^-$			
μ_{cc}	0.01	0.001	0.0001	μ_{cc}	0.01	0.001	0.0001
$N\eta_c$	ub	ub	ub	NJ/ψ	ub	ub	ub
NJ/ψ	ub	ub	ub	$\Lambda_c D^*$	ub	ub	ub
$\Lambda_c D$	ub	ub	ub	$\Sigma_c D^*$	-16/4446	-11/4451	-10/4452
$\Lambda_c D^*$	ub	ub	ub	$\Sigma_c^* D$	-17/4367	-14/4370	-12/4372
$\Sigma_c D$	−19/4300	−15/4304	−13/4306	$\Sigma_c^* D^*$	−17/4510	−15/4512	−13/4514
$\Sigma_c D^*$	−21/4441	−19/4443	−18/4444	$J^P = \frac{5}{2}^-$			
$\Sigma_c^* D^*$	−24/4503	−23/4504	−21/4506	$\Sigma_c^* D^*$	−15/4512	−10/4517	−10/4517

≠ **Pc(4450)**

Pc(4380)

Comparing with the LHCb's result in 2015

- ✓ The main component of the Pc(4380) maybe Σc*D with J^P = $3/2^-$.
- ✓ The mass of the ΣcD* with J^P = $3/2^-$ is close to the reported Pc(4450), but the opposite parity of this state to Pc(4380) may prevent one from making this assignment at that time.

• The channel-coupling calculation

Table 6 The masses (in MeV) of the hidden-charm molecular pentaquarks with all channels coupling and the percentages of each channel in the eigen-states

$J^P = \frac{1}{2}^-$				$J^P = \frac{3}{2}^-$				$J^P = \frac{5}{2}^-$			
μ_{cc}	0.01	0.001	0.0001	μ_{cc}	0.01	0.001	0.0001	μ_{cc}	0.01	0.001	0.0001
M_{cc}	3881	3883	3884	M_{cc}	3997	3998	3998	M_{cc}	4512	4517	4517
$N\eta_c$	41.7	49.7	35.2	NJ/ψ	80.8	71.0	62.1	$\Sigma_c^* D^*$	100.0	100.0	100.0
NJ/ψ	23.1	24.4	29.3	$\Lambda_c D^*$	8.7	11.9	15.9				
$\Lambda_c D$	14.6	11.7	14.5	$\Sigma_c D^*$	1.2	1.9	2.6				
$\Lambda_c D^*$	0.9	0.4	2.0	$\Sigma_c^* D$	3.5	5.8	7.3				
$\Sigma_c D$	0.1	4.8	6.0	$\Sigma_c^* D^*$	5.8	9.4	12.1				
$\Sigma_c D^*$	4.5	6.4	12.4								
$\Sigma_c^* D^*$	15.1	2.6	0.6								

- ✓ A bound state: $J^P = 1/2^-$ Nηc
- ✓ $J^P = 3/2^-$ NJ/ψ (*decay to open channels: D−wave Nηc*)
- ✓ $J^P = 5/2^-$ Σc*D* (*decay to open channels: some D−wave channels*)
- ✓ Where are these states?

$J^P = 1/2^-$ ΣcD, ΣcD*, Σc*D* *(decay to open channels: S-wave Nηc, NJ/ψ, ΛcD, ΛcD* and some D-wave channels)*

$J^P = 3/2^-$ Σc∗D, ΣcD∗, Σc*D* *(decay to open channels: S−wave NJ/ψ, ΛcD∗ and some D−wave channels)*

They maybe the resonance states.

To check whether they are resonance states or not, the study of scattering process of the corresponding open channels are needed !

- Resonance states in the scattering process

1. $J^P = 1/2^-$

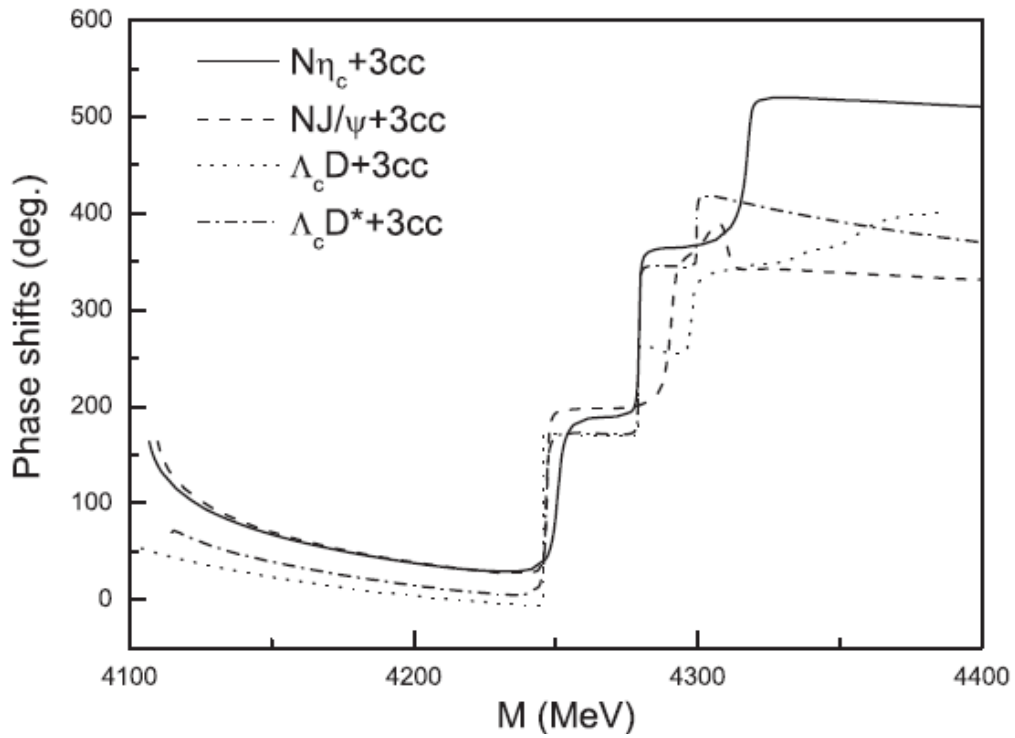

FIG. 2. The $N\eta_c$, NJ/ψ, $\Lambda_c D$, and $\Lambda_c D^*$ S-wave phase shifts with four-channel coupling for the $IJ^P = \frac{1}{2}\frac{1}{2}^-$ system.

- There are three resonance states: ΣcD, ΣcD*, and Σc*D* in the Nηc scattering phase shifts.
- In other scattering channels there are only two resonance states: ΣcD and ΣcD*.
- There is only a cusp around the threshold of the third state Σc*D*, because the channel coupling pushes the higher state above the threshold.

TABLE II. The masses and decay widths (in MeV) of the $IJ^P = \frac{1}{2}\frac{1}{2}^-$ resonance states in the $N\eta_c$, NJ/ψ, $\Lambda_c D$, and $\Lambda_c D^*$ S-wave scattering process.

	Two-channel coupling						Four-channel coupling					
	$\Sigma_c D$		$\Sigma_c D^*$		$\Sigma_c^* D^*$		$\Sigma_c D$		$\Sigma_c D^*$		$\Sigma_c^* D^*$	
	M'	Γ_i	M'	Γ_i	M'	Γ_i	M'	Γ_i	M'	Γ_i	M'	Γ_i
$N\eta_c$	4312.9	6.0	4451.7	1.1	4523.1	3.5	4311.3	4.5	4448.8	1.0	4525.8	4.0
NJ/ψ	4309.9	2.0	4461.6	4.0	4514.7	1.2	4307.9	1.2	4459.7	3.9	nr	⋯
$\Lambda_c D$	4308.4	0.003	4452.6	1.0	4512.6	0.004	4306.7	0.02	4461.6	1.0	nr	⋯
$\Lambda_c D^*$	4311.6	3.5	4452.5	1.0	4510.8	0.005	4307.7	1.4	4449.0	0.3	nr	⋯
Γ_{total}		11.5		7.1		4.7		7.1		6.2		4.0

Pc(4312) **Pc(4457)**

2. $J^P = 3/2^-$

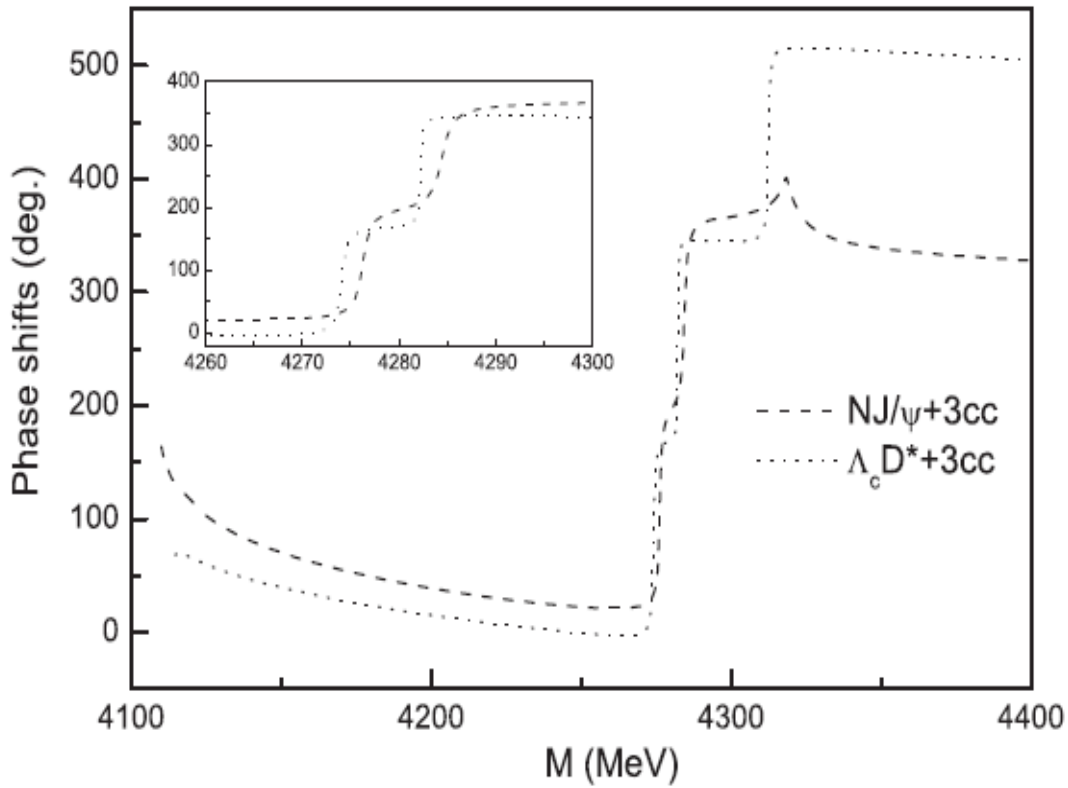

FIG. 4. The NJ/ψ and $\Lambda_c D^*$ S-wave phase shifts with four-channel coupling for the $IJ^P = \frac{1}{2}\frac{3}{2}^-$ system.

- There are two resonance states: ΣcD* and Σc*D in the NJ/ψ scattering phase shifts.
- There are three resonance states: ΣcD*, Σc*D and Σc*D* in the ΛcD* scattering phase shifts.

TABLE III. The masses and decay widths (in MeV) of the $IJ^P = \frac{1}{2}\frac{3}{2}^-$ resonance states in the NJ/ψ and $\Lambda_c D^*$ S-wave scattering process.

	Two-channel coupling					
	$\Sigma_c D^*$		$\Sigma_c^* D$		$\Sigma_c^* D^*$	
	M'	Γ_i	M'	Γ_i	M'	Γ_i
NJ/ψ	4453.8	1.7	4379.7	4.5	4526.4	2.5
$\Lambda_c D^*$	4452.7	0.8	4377.6	3.2	4522.7	1.8
Γ_{total}		2.5		7.7		4.3

	Four-channel coupling					
	$\Sigma_c D^*$		$\Sigma_c^* D$		$\Sigma_c^* D^*$	
	M'	Γ_i	M'	Γ_i	M'	Γ_i
NJ/ψ	4445.7	1.5	4376.4	1.5	nr	...
$\Lambda_c D^*$	4444.0	0.3	4374.4	0.9	4523.0	1.0
Γ_{total}		1.8		2.4		1.0

?

Pc(4440) **Pc(4380)**

- Compare with the experiment

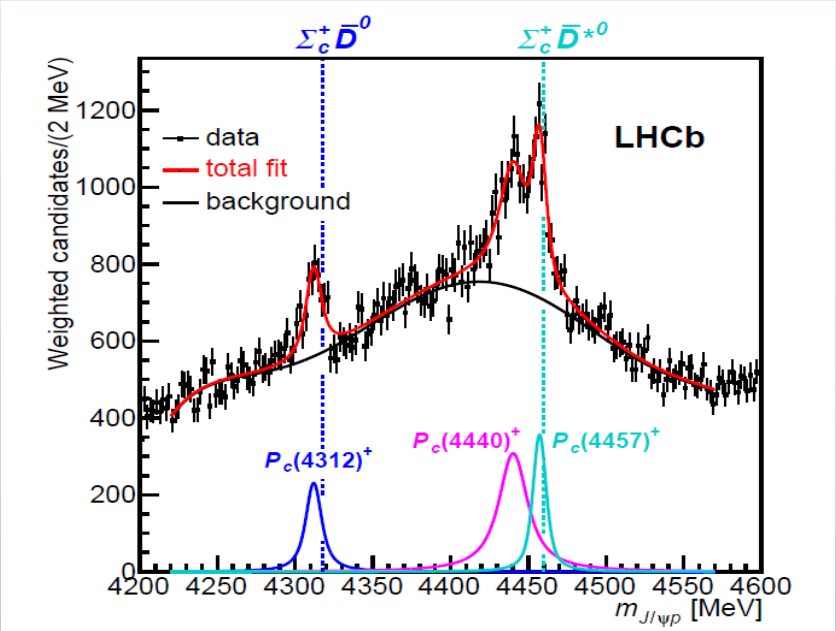

Figure 6: Fit to the $\cos\theta_{P_c}$-weighted $m_{J/\psi p}$ distribution with three BW amplitudes and a sixth-order polynomial background. This fit is used to determine the central values of the masses and widths of the P_c^+ states. The mass thresholds for the $\Sigma_c^+\bar{D}^0$ and $\Sigma_c^+\bar{D}^{*0}$ final states are superimposed.

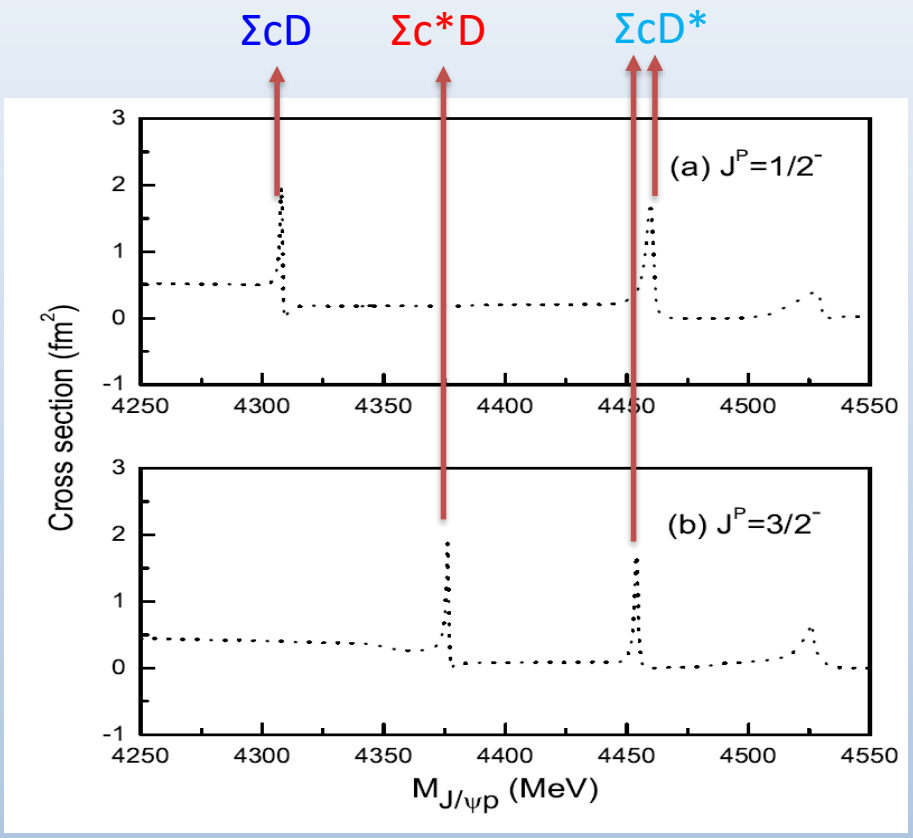

LHCb Collaboration,
Phys. Rev. Lett. 122 222001 (2019)

Phys. Rev. D. 99, 014010 (2019),
arXiv: 1904.00221

IV. Hidden-bottom pentaquarks

1. $J^P = 1/2^-$

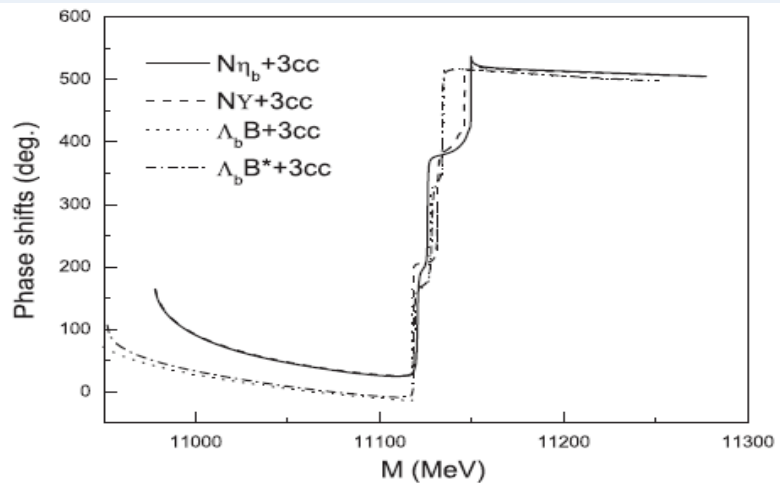

FIG. 6. The $N\eta_b$, $N\Upsilon$, $\Lambda_b B$ and $\Lambda_b B^*$ S-wave phase shifts with four-channel coupling for the $IJ^P = \frac{1}{2}\frac{1}{2}^-$ system.

TABLE IV. The masses and decay widths (in MeV) of the $IJ^P = \frac{1}{2}\frac{1}{2}^-$ resonance states in the $N\eta_b$, $N\Upsilon$, $\Lambda_b B$, and $\Lambda_b B^*$ S-wave scattering process.

	Two-channel coupling						Four-channel coupling					
	$\Sigma_b B$		$\Sigma_b B^*$		$\Sigma_b^* B^*$		$\Sigma_b B$		$\Sigma_b B^*$		$\Sigma_b^* B^*$	
	M'	Γ_i	M'	Γ_i	M'	Γ_i	M'	Γ_i	M'	Γ_i	M'	Γ_i
$N\eta_b$	11 083.3	4.0	11 123.9	1.4	11 154.5	4.7	11 079.8	1.2	11 120.6	0.4	11 156.9	2.0
$N\Upsilon$	11 080.4	1.4	11 135.4	6.6	11 146.2	2.0	11 077.5	0.1	11 125.8	0.8	11 153.5	3.0
$\Lambda_b B$	11 079.0	0.000 3	11 125.4	2.0	11 145.1	0.49	11 077.2	0.001	11 122.0	0.6	11 141.8	0.1
$\Lambda_b B^*$	11 082.2	2.6	11 126.2	2.3	11 142.7	0.22	11 078.3	0.3	11 123.0	1.2	11 141.5	0.4
Γ_{total}		7.0		12.3		7.4		1.6		3.0		5.5

2. $J^P = 3/2^-$

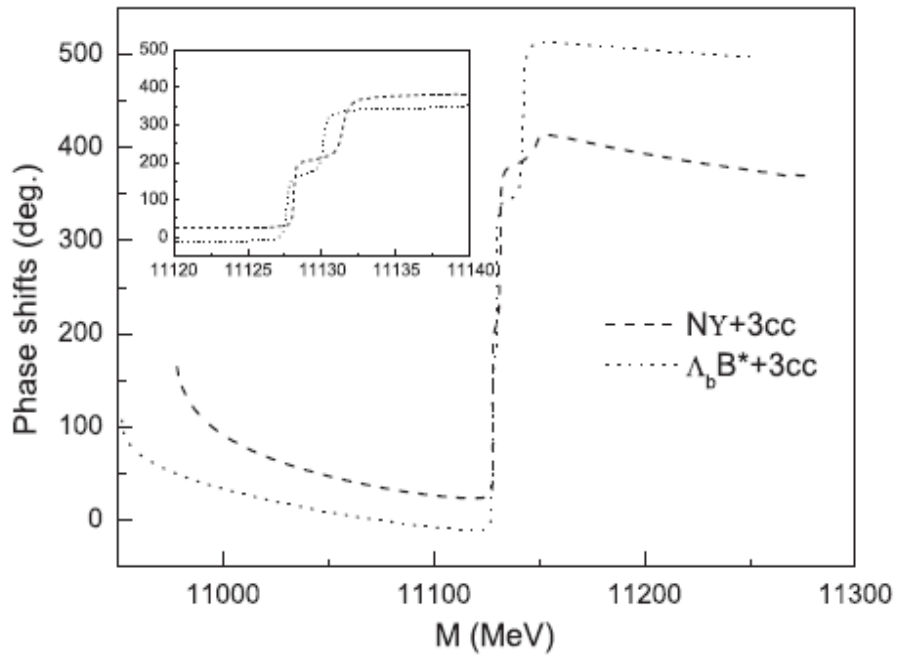

FIG. 8. The $N\Upsilon$ and $\Lambda_b B^*$ S-wave phase shifts with four-channel coupling for the $IJ^P = \frac{1}{2}\frac{3}{2}^-$ system.

TABLE V. The masses and decay widths (in MeV) of the $IJ^P = \frac{1}{2}\frac{3}{2}^-$ resonance states in the $N\Upsilon$ and $\Lambda_b B^*$ S-wave scattering process.

	Two-channel coupling					
	$\Sigma_b B^*$		$\Sigma_b^* B$		$\Sigma_b^* B^*$	
	M'	Γ_i	M'	Γ_i	M'	Γ_i
$N\Upsilon$	11 126.3	1.7	11 105.8	4.4	11 155.7	3.8
$\Lambda_b B^*$	11 125.5	0.9	11 103.5	2.6	11 152.0	2.7
Γ_{total}		2.6		7.0		6.5
	Four-channel coupling					
	$\Sigma_b B^*$		$\Sigma_b^* B$		$\Sigma_b^* B^*$	
	M'	Γ_i	M'	Γ_i	M'	Γ_i
$N\Upsilon$	11 122.7	0.2	11 103.6	0.8	nr	...
$\Lambda_b B^*$	11 122.2	0.2	11 102.4	0.3	11 150.0	1.8
Γ_{total}		0.4		1.1		1.8

- ✓ The results are similar to the hidden-charm pentaquarks.
- ✓ Some narrow hidden-bottom pentaquark resonances above 11 GeV are found from corresponding scattering process.

V. Hidden-strange pentaquarks

- The hidden strange pentaquark channels

TABLE II. The coupling channels of each quantum number.

J^P	$^{2S+1}L_J$	Channels
$\frac{1}{2}^-$	$^2S_{\frac{1}{2}}$	$N\eta'$, $N\phi$, ΛK, ΛK^*, ΣK, ΣK^*, $\Sigma^* K^*$
	$^4D_{\frac{1}{2}}$	$N\phi$, ΛK^*, ΣK^*, $\Sigma^* K$, $\Sigma^* K^*$
$\frac{3}{2}^-$	$^2D_{\frac{3}{2}}$	$N\eta'$, $N\phi$, ΛK, ΛK^*, ΣK, ΣK^*, $\Sigma^* K^*$
	$^4S_{\frac{3}{2}}(^4D_{\frac{3}{2}})$	$N\phi$, ΛK^*, ΣK^*, $\Sigma^* K$, $\Sigma^* K^*$
$\frac{5}{2}^-$	$^2D_{\frac{5}{2}}$	$N\eta'$, $N\phi$, ΛK, ΛK^*, ΣK, ΣK^*, $\Sigma^* K^*$
	$^4D_{\frac{5}{2}}$	$N\phi$, ΛK^*, ΣK^*, $\Sigma^* K$, $\Sigma^* K^*$
$\frac{1}{2}^+$	$^2P_{\frac{1}{2}}$	$N\eta'$, $N\phi$, ΛK, ΛK^*, ΣK, ΣK^*, $\Sigma^* K^*$
	$^4P_{\frac{1}{2}}$	$N\phi$, ΛK^*, ΣK^*, $\Sigma^* K$, $\Sigma^* K^*$
$\frac{3}{2}^+$	$^2P_{\frac{3}{2}}$	$N\eta'$, $N\phi$, ΛK, ΛK^*, ΣK, ΣK^*, $\Sigma^* K^*$
	$^4P_{\frac{3}{2}}$	$N\phi$, ΛK^*, ΣK^*, $\Sigma^* K$, $\Sigma^* K^*$
$\frac{5}{2}^+$	$^4P_{\frac{5}{2}}$	$N\phi$, ΛK^*, ΣK^*, $\Sigma^* K$, $\Sigma^* K^*$

✓ The states of P and D wave are unbound in present calculations.

- The effective potentials

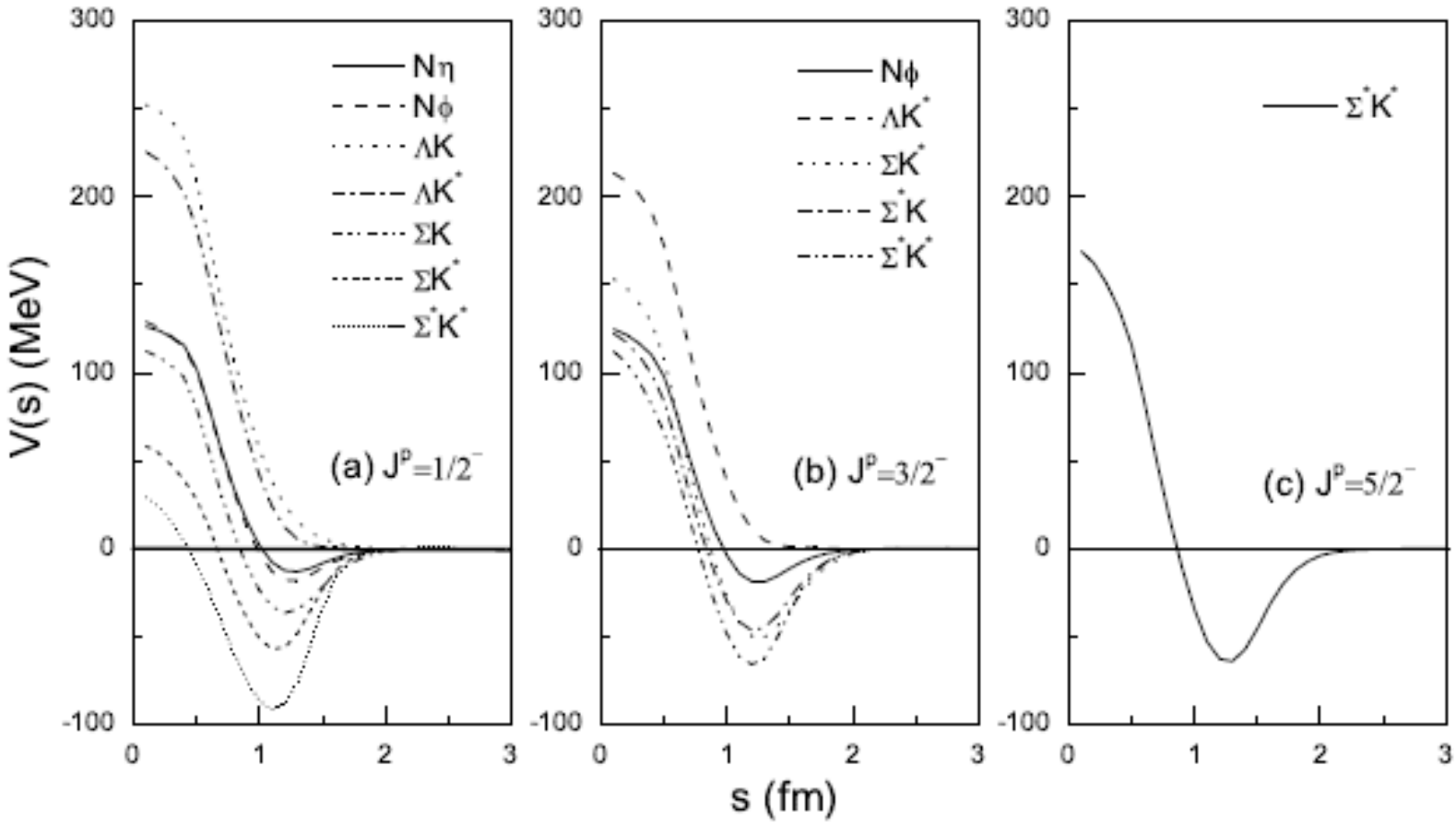

FIG. 1: The potentials of different channels for the $I = \frac{1}{2}$, $J^P = \frac{1}{2}^-, \frac{3}{2}^-, \frac{5}{2}^-$ systems.

- The bound state calculation

TABLE III. The binding energy and the total energy of each individual channel and all coupled channels for the two S-wave bound states with the quantum numbers $J^P = \frac{1}{2}^-$ and $\frac{3}{2}^-$. The values are provided in units of MeV, and "ub" represents unbound.

Channel	$J^P = \frac{1}{2}^-$			$J^P = \frac{3}{2}^-$		
	QDCSM1	QDCSM2	QDCSM3	QDCSM1	QDCSM2	QDCSM3
$N\eta'$	ub	ub	ub	–	–	–
$N\phi$	ub	ub	ub	ub	ub	ub
ΛK	ub	ub	ub	–	–	–
ΛK^*	ub	ub	ub	ub	ub	ub
ΣK	−6.7/1681.3	−26.8/1661.2	−4.9/1683.1	–	–	–
ΣK^*	−8.9/2076.1	−30.6/2054.4	−22.4/2062.2	−21.6/2063.4	−21.1/2063.9	−21.2/2063.8
$\Sigma^* K$	–	–	–	−10.4/1869.6	−15.5/1864.5	−11.1/1868.9
$\Sigma^* K^*$	−17.3/2259.7	−87.0/2190.0	−73.9/2203.1	−11.3/2265.7	−18.4/2258.6	−27.2/2249.8
Coupled	−16.0/1881.0	−20.0/1877.0	−24.3/1872.7	−10.1/1948.9	−7.7/1951.3	−1.6/1957.4

- ✓ Nη' is a bound state by channel-coupling calculation.
- ✓ Nϕ may be a resonance state.

- Resonance states in the scattering process

1. Nϕ

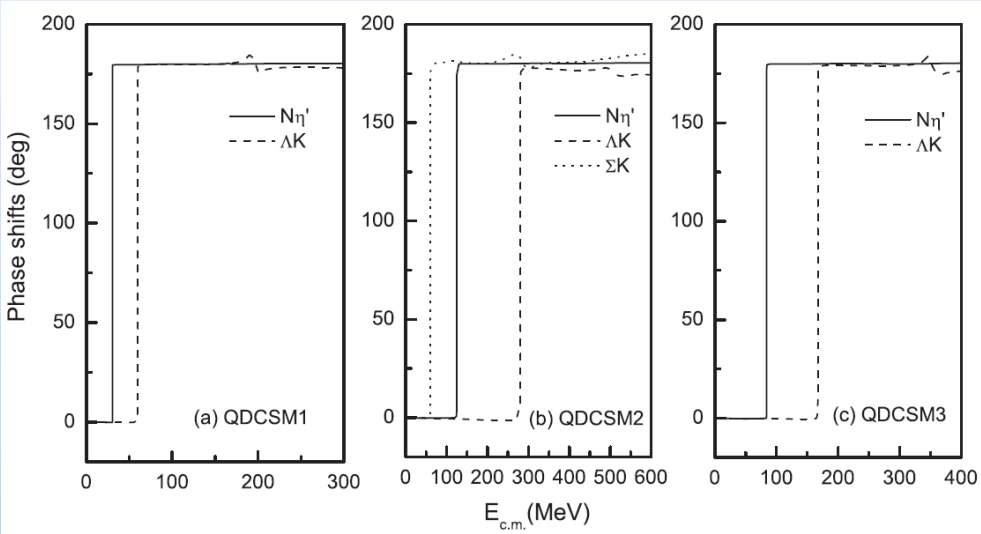

FIG. 1. The phase shifts of different scattering channels for the $J^P = \frac{3}{2}^-$ systems.

TABLE IV. The $N_{s\bar{s}}$ bound state mass calculated from the $^2D_{\frac{3}{2}}$ scattering channels. The values are provided in units of MeV.

Scattering channel	QDCSM1	QDCSM2	QDCSM3
$N\eta'$	1947.998	1949.485	1955.988
ΛK	1947.975	1949.480	1955.910
ΣK	–	1949.597	–

TABLE V. The decay widths and branch ratios of each decay channel of $N_{s\bar{s}}$ bound state.

Decay channel	QDCSM1		QDCSM2		QDCSM3	
	Γ_i(MeV)	Γ_i/Γ(%)	Γ_i(MeV)	Γ_i/Γ(%)	Γ_i(MeV)	Γ_i/Γ(%)
$N\eta'$	0.002	0.1	0.022	0.5	0.009	0.2
ΛK	0.011	0.3	0.120	2.9	0.055	1.2
ΣK	–	0.0	0.060	1.5	–	0.0
ϕ decays	3.619	99.6	3.892	95.1	4.616	98.6

2. Pc-like resonances

TABLE IV. The resonance mass and decay width (in MeV) of the molecular pentaquarks with $J^P = \frac{1}{2}^-$.

	ΣK		ΣK^*		$\Sigma^* K^*$	
S wave	M_r	Γ_i	M_r	Γ_i	M_r	Γ_i
$N\eta'$	···	···	2079.4	1.1	2246.8	20.0
$N\phi$	···	···	2080.0	3.6	2237.0	30.0
ΛK	1668.0	1.3	2083.4	1.0	2261.5	20.0
ΛK^*	···	···	2056.6	0.2	2219.0	58.0
ΣK	···	···	2071.6	4.6	2252.3	6.0
ΣK^*	···	···	···	···	2253.9	16.0
D wave						
$N\phi$	···	···	2076.3	0.3	2254.4	0.006
ΛK^*	···	···	2076.3	0.4	2253.6	0.6
ΣK^*	···	···	···	···	2254.0	0.06
$\Sigma^* K$	···	···	2076.8	0.01	2253.3	0.8

TABLE V. The resonance mass and decay width (in MeV) of the molecular pentaquarks with $J^P = \frac{3}{2}^-$.

	ΣK^*		$\Sigma^* K$		$\Sigma^* K^*$	
S wave	M_r	Γ_i	M_r	Γ_i	M_r	Γ_i
$N\phi$	2060.6	10.4	···	···	2270.5	0.03
ΛK^*	2046.1	15.0	···	···	2256.5	2.0
ΣK^*	···	···	···	···	2270.6	0.1
$\Sigma^* K$	2054.1	2.3	···	···	2263.6	3.7
D wave						
$N\eta'$	2061.4	0.001	1875.7	0.0004	2269.2	0.01
$N\phi$	2061.0	0.2	···	···	2269.3	0.01
ΛK	2060.6	0.9	1871.6	0.08	2269.2	0.02
ΛK^*	2059.1	0.3	···	···	2269.1	0.05
ΣK	2060.3	0.9	1871.6	0.05	2269.2	0.02
ΣK^*	···	···	···	···	2269.2	0.003

N*(2100) **N*(1875)**

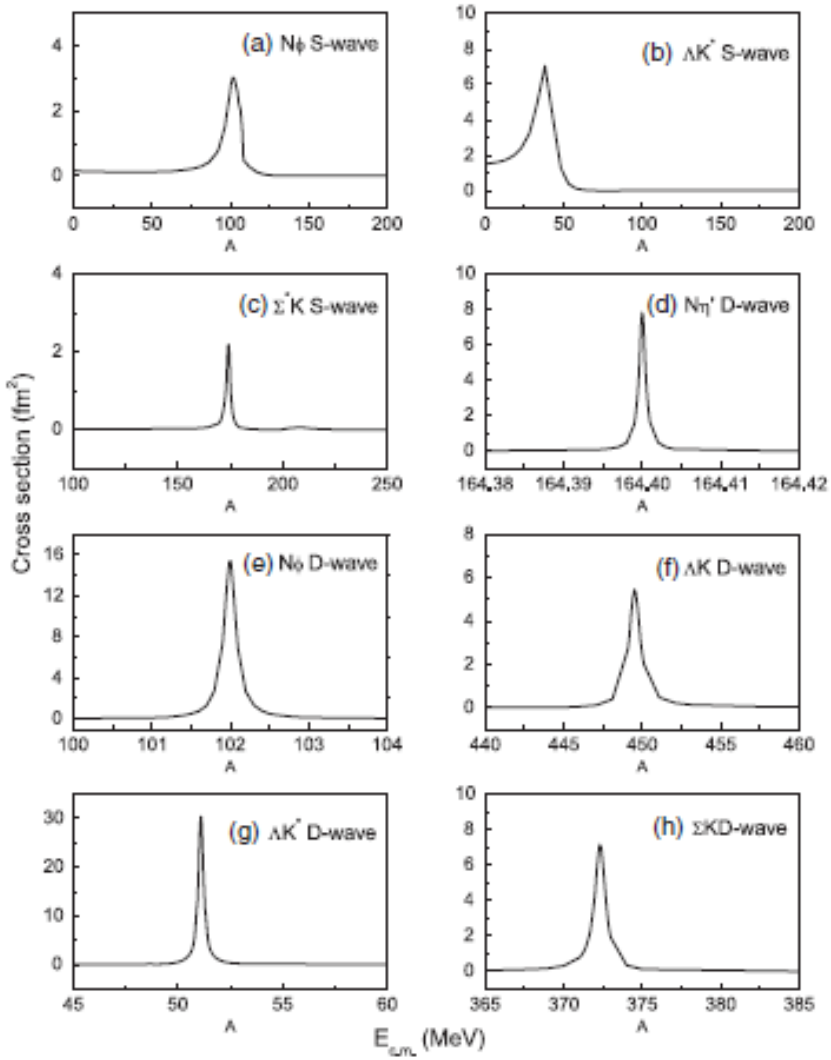

FIG. 2. The cross section of all open channels for the state ΣK^* with $J^P = \frac{3}{2}^-$.

VI. Summary

1. Hidden-strange pentaquark

1 bound state: $J^P = 1/2^-$ Nη'

8 resonance states: $J^P = 1/2^-$ ΣK, ΣK*, Σ*K*

$J^P = 3/2^-$ Σ∗K (N*(1875)), ΣK∗(N*(2100)), Σ∗K∗, Nϕ

$J^P = 5/2^-$ Σ*K*

2. Hidden-charm pentaquark

1 bound state: $J^P = 1/2^-$ Nηc

8 resonance states: $J^P = 1/2^-$ ΣcD (Pc(4312)), ΣcD* (Pc(4457)), Σc*D*

$J^P = 3/2^-$ Σc∗D (Pc(4380)), ΣcD∗ (Pc(4440)), Σc∗D∗, NJ/ψ

$J^P = 5/2^-$ Σc*D*

3. Hidden-bottom pentaquark

1 bound state: $J^P = 1/2^-$ Nηb

8 resonance states: $J^P = 1/2^-$ ΣbB, ΣbB*, Σb*B*

$J^P = 3/2^-$ Σb∗B, ΣbB∗, Σb∗B∗, NY

$J^P = 5/2^-$ Σb*B*

Thanks for your attention!